NEUROPATHOLOGY

Neuropathology 2020 doi:10.1111/neup.12672

Case Report

High-grade gliomas with isocitrate dehydrogenase wild-type and 1p/19q codeleted: Atypical molecular phenotype and current challenges in molecular diagnosis

Linmao Zheng, Mengni Zhang, Jing Hou, Jing Gong, Ling Nie, Xueqin Chen, Qiao Zhou and Ni Chen

Pathology Department and State Key Laboratory of Biotherapy, West China Hospital, Sichuan University, Chengdu, China

Glioma is the most common intracranial malignant tumor, with poor prognosis. The new World Health Organization (WHO) integrated classification (2016) for diffuse glioma is mainly based on the status of the isocitrate dehydrogenase (IDH) gene (*IDH*) mutation and 1p/19q codeletion, with diffuse glioma separated into three distinct molecular categories: chromosome 1p/19q codeletion/*IDH* mutant, 1p/19q intact /*IDH* mutant, and *IDH* wild-type. Gliomas harboring 1p/19q codeletion but without *IDH* mutation are rare and cannot be classified according to the new revision of the WHO classification. Here we report three high-grade gliomas with this atypical molecular phenotype, and describe their histological and immunohistochemical features, the status of mutations in *TERT* promopter, *H3F3A, HIST1H3B*, and *BRAF*, as well as *MGMT* promoter methylation, and prognosis. Considering morphology, molecular parameters, and patients prognosis, we found that high-grade gliomas harboring 1p/19q codeletion but without *IDH* mutation were not typical glioblastoma multiforme (GBM) but were more likely to be GBM than anaplastic oligodendroglioma.

Key words: 1p/19q codeletion, atypical molecular phenotype, glioma, IDH mutation, molecular diagnosis.

INTRODUCTION

Glioma is the most common intracranial malignant tumor, and has a poor prognosis.[1] Grade I and II gliomas are low-grade, while grade III and IV gliomas are high-grade, the latter two having worse outcomes.[2] Previously, diagnosis of gliomas was completely based on morphology. Recent developments in molecular analysis have revealed many genetic alterations in gliomas. The World Health Organization (WHO) 2016 classification of tumors of the central nervous system (CNS) breaks the century-old principle of diagnosis based entirely on histology by integrating molecular information into the classification of CNS tumors. This new integrated classification for diffuse glioma is mainly based on the status of the isocitrate dehydrogenase (IDH) gene (*IDH*) mutation and 1p/19q codeletion, which separate diffuse glioma into three distinct molecular categories: chromosome 1p/19q codeletion/IDH mutant, 1p/19q intact /*IDH* mutant, and *IDH* wild-type. In the new classification, oligodendrogliomas are defined as diffusely infiltrating gliomas with *IDH1* and *IDH2* mutation and 1p/19q codeletion.[3,4]

Other molecular biomarkers, including the telomerase reverse transcriptase (TERT) gene (*TERT*) promoter mutation, *H3K27* mutation, *BRAF* mutation, and *MGMT* promoter methylation, have been widely used for diagnosis, treatment, and prognosis prediction of gliomas.[5] Promoter mutation in *TERT*[6,7] and promoter methylation in *MGMT*[8,9] are also present in the vast majority of oligodendrogliomas. Loss of alpha thalassemia/mental retardation syndrome X-linked (ATRX) protein expression is mutually exclusive of 1p/19q codeletion.[10] Strong and diffuse nuclear p53 staining is commonly seen in glioblastoma multiforme (GBM).[11]

The 1p/19q codeletion is the most important genetic characteristics of oligodendroglioma. According to some studies, typical 1p/19q codeletion is always associated with *IDH* mutation.[12,13] However, gliomas with 1p/19q codeletion but without *IDH* mutation have also been reported, with an incidence rate of approximately 0.2% to

Correspondence: Dr Ni Chen, Pathology Department, West China Hospital, Sichuan University, Chengdu, 610041, China. Tel: 86-28-85422701. Email: chenni1@163.com

Received 29 October 2019; revised 09 January 2020; accepted 15 January 2020.

0.4%.[14–16] None of these special cases have undergone multigenetic comprehensive molecular testing, like *TERT* promoter mutation and *MGMT* promoter methylation, or have been analyzed in previous studies. Therefore, it is difficult to classify these gliomas.

In the present study, we reported three high-grade glioma cases showing IDH wild-type and 1p/19q codeletion. Here we comprehensively describe their clinical and histological features, immunohistochemical phenotype, and other molecular characteristics, such as the status of mutations in *TERT* promotor, *H3F3A, HIST1H3B*, and *BRAF* as well as *MGMT* promotor methylation, and discuss the appropriate classification for this type of gray area glioma.

CASE REPORT

Case 1

A 38-year-old woman presented with recurrent headaches for three years and had a history of seizure one month before. She had a progressive headache with non-projectile vomiting for 15 days. Magnetic resonance imaging (MRI) revealed a hyperintense mass in the right frontal lobe on T1-weighted images (T1WIs) and T2WIs (Fig. 1A, B). A few plaque-like edema zones with hypointensity on the T1WIs and hyperintensity on fluid-attenuated inversion recovery (FLAIR) images (Fig. 1C) were seen. Gadolinium-contrast T1WIs showed that the periphery of the tumor was intensely enhanced (Fig. 1D). The mass was surgically excised. The patient refused adjuvant radiotherapy and chemotherapy after the operation and died nine months after the operation.

Case 2

A 63-year-old man with a progressive headache for ten days was admitted to our hospital. MRI revealed a lesion involving the right temporal and parietal lobes, which was considered a high-grade glioma. After the operation, he received radiotherapy, accompanied by a long period of temozolomide (TMZ) adjuvant therapy. However, six months later, the tumor relapsed and progressed with multiple intracranial metastases. He died 12 months after the operation.

Case 3

A 48-year-old man was transferred to our hospital complaining of numbness and only being able to write slowly with his right hand. MRI revealed an ill-defined mass with heterogeneously enhanced areas in the left parietal lobe. He received gross total resection of the mass and standard TMZ chemotherapy. At the time writing this paper, only two months had passed since the operation, and no evidence of local recurrence or distant metastasis was found.

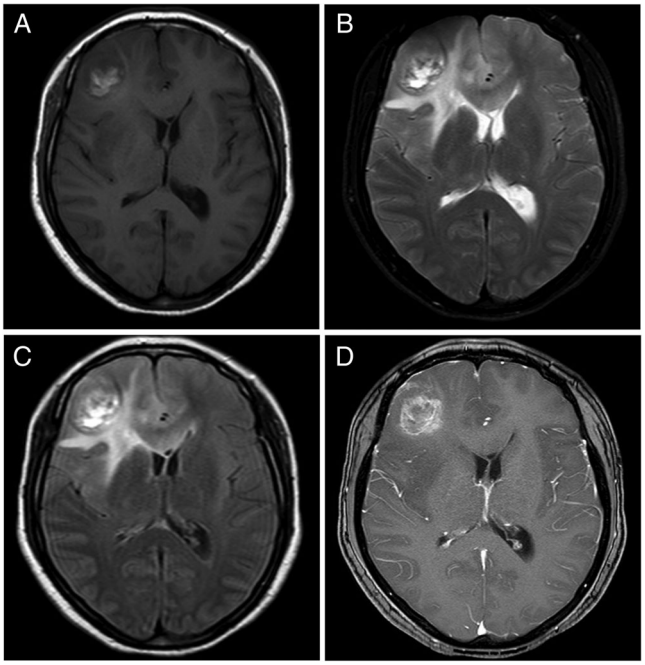

Fig 1 MRI findings of the brain. A T1WI (A) and a T2WI (B) exhibit a hyperintense mass in the right frontal lobe. The anterior horn of the right ventricle is compressed by the mass, and the midline is shifted to the left side. A few plaque-like edema zones with hypointensity on the T1WI (A) and hyperintensity on an FLAIR image (C) are seen. A Gadolinium-contrast T1WI shows that the periphery of the tumor is intensely enhanced (D).

MATERIALS AND METHODS

Materials

Archived formalin-fixed, paraffin-embedded (FFPE) specimens were used for histopathological, immunohistochemical, and molecular analyses. All materials were used in accordance with institution-approved ethical guidelines and procedures.

Immunohistochemistry

For immunohistochemistry, we used the primary antibodies against IDH1 R132H (mouse monoclonal, clone H09; Dianova, Germany), p53 (mouse monoclonal, clone DO-7; DakoCytomation, Glostrup, Denmark), Ki-67 (mouse monoclonal, clone MIB-1; DakoCytomation), glial fibrillary acidic protein (GFAP) (rabbit monoclonal, clone EP13; Zhongshan, Beijing, China), Oligo2 (rabbit monoclonal, clone EP112; Zhongshan), ATRX (rabbit polyclonal, ZA-0016; Zhongshan), epithelial membrane antigen (EMA) (mouse monoclonal, clone E29; DakoCytomation) NeuN (mouse monoclonal A60; Zhongshan), and H3 K27M (rabbit monoclonal, clone RM192; Zhongshan). Immunoreaction product deposits were visualized by the polymer-immunocomplex method using an Envision System

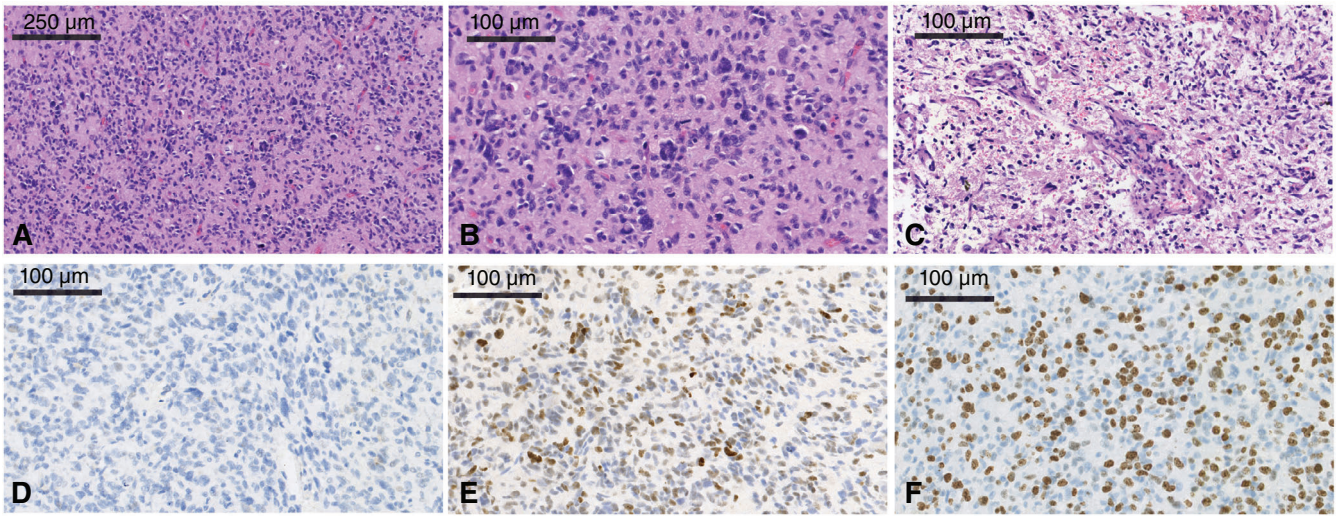

Fig 2 Histological (A, B) and immunohistochemical (C-F) findings in case 1. Low-power view of a section stained with HE shows high cellularity (A). High-power view of the HE-stained section shows nuclear pleomorphism, marked nuclear atypia (B), and microvascular proliferation (C). Tumor cells are negatively immunostained for IDH1 R132H (D). Approximately 30% of the tumor cells are moderately positive for nuclear p53 (E). The Ki-67 labeling index is about 40% (F).

(DakoCytomation) according to the manufacturer's protocols. Histological findings were observed on sections stained with hematoxylin and eosin (HE).

Fluorescence *in situ* hybridization

Fluorescence *in situ* hybridization (FISH) was performed by using dual-color 1p36/1q25 and 19q13/19p13 probes (Vysis, Downers Grove, IL, USA). Briefly, FFPE sections were deparaffinized, permeabilized, and hybridized. Samples with bright signals for both probe sets in greater than 90% of nuclei were considered acceptable. One-hundred nonoverlapping nuclei were scored for signals from the probes 1p36 (red)/1q25 (green) and 19q13 (red)/19p13 (green) with a fluorescence microscope. An interpretation of deletion was made when 30% of the nuclei or more displayed only one red and two green signals.

Next-generation sequencing-based target single-nucleotide polymorphism analysis

Next-generation sequencing (NGS) was performed using a Genetron Health (Beijing, China) according to the manufacturer's protocols. Single-nucleotide polymorphism (SNP) of chromosomes 1p and 19q was

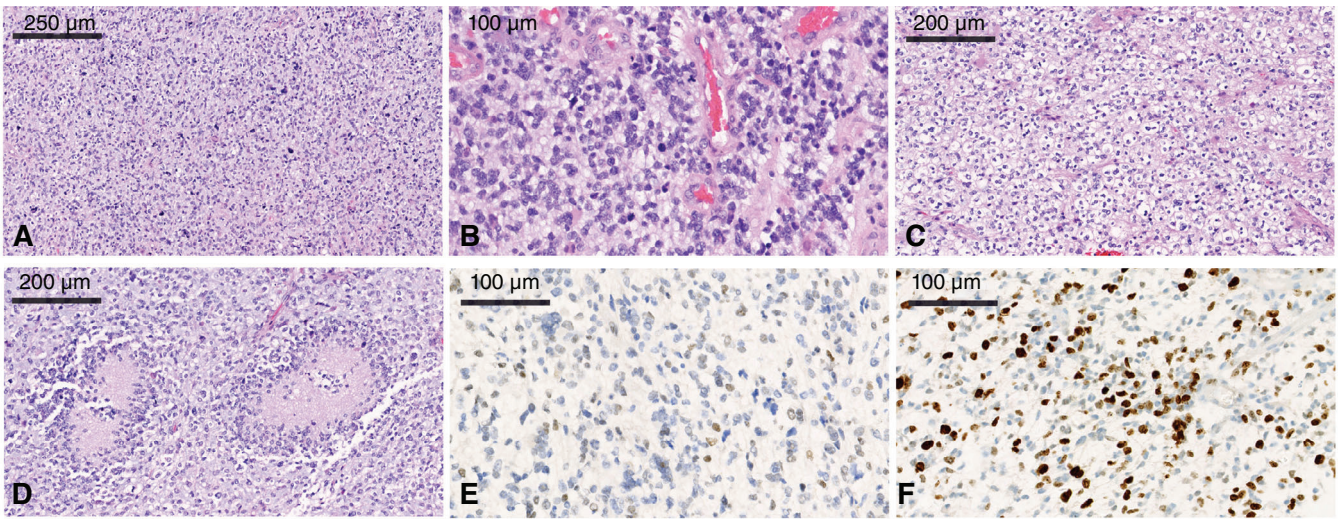

Fig 3 Histological (A, B) and immunohistochemical (C-F) findings in case 2. Low-power view of a section stained with HE shows high cellularity and nuclear pleomorphism (A). High-power view of the HE-stained section shows nuclear pleomorphism and brisk mitotic activity (B). A focal oligodendroglima component (C) and a specific neuropil-like island structure (D) are also seen. This tumor lacked strong and diffuse nuclear p53 immunostaining (E) and the Ki-67 labeling index is about 30% (F).

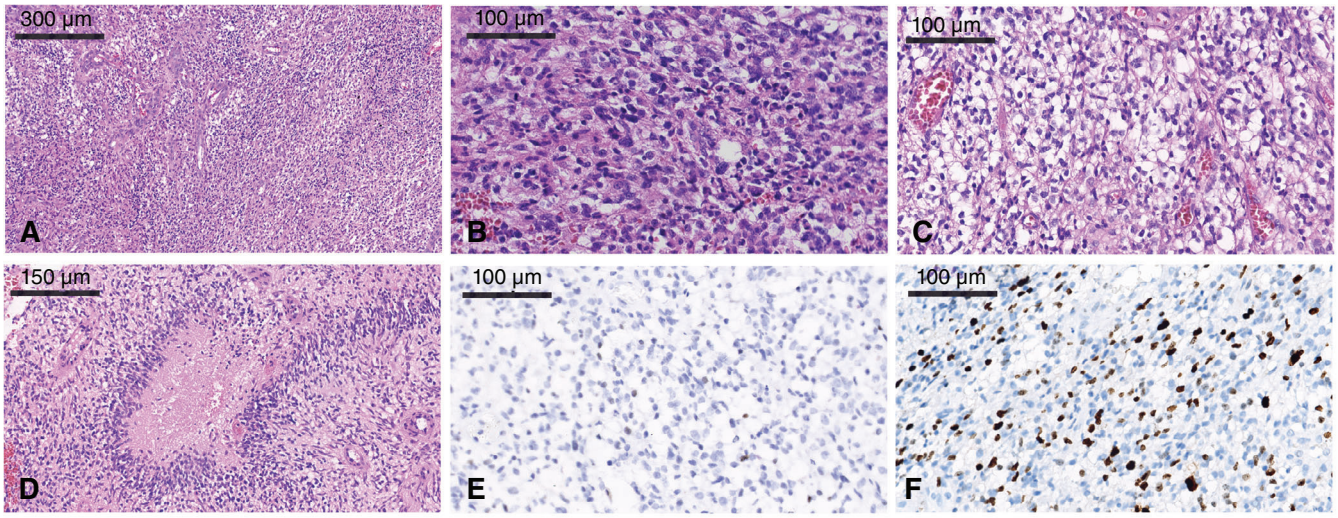

Fig 4 Hisotlogical (A, B) and immunohistochemical (C-F) findings in case 3. Low-power view of a section stained with HE shows the high cellularity and microvascular proliferation (A). High-power view of the HE-stained section shows nuclear pleomorphism and brisk mitotic activity (B). Appearance of a focal oligodendroglioma-like component (C) and palisading necrosis (D) are also seen in this tumor. Nearly no immunostaining for p53 is observed in this tumor (E). The Ki-67 labeling index is approximately 25% (F).

detected by NGS according to the literature. Twenty-eight target SNPs on chromosome 1p and 32 target SNPs on chromosome 19q were selected, respectively. When a normal sample was examined, the B-allele frequency varied from 35% to 65%, and the homozygous reference and homozygous variant were located close to allele frequencies of 0% and 100%, respectively. When a sample with 1p or 19q deletion was examined, the B-allele frequency deviated.[17]

Polymerase chain reaction-based Sanger sequencing

Total DNA was isolated using a TaKaRa Dexpat Kit (TaKaRa Bio, Kyoto, Japan) according to the manufacturer's instructions. The polymerase chain reaction (PCR) primers were designed as follows: *IDH1* (forward, 5′-CGG TCT TCA GAG AAG CCA TT-3′; reverse, 5′-GCA AAA TCA CAT TAT TGC CAA C-3′, 129 bp), *IDH2* (forward, 5′-AGC CCA TCA TCT GCA AAA AC-3′; reverse, 5′-CTA GGC GAG GAG CTC CAG T-3′, 150 bp), *H3F3A* (forward, 5′-GTA CAA AGC AGA CTG CCC GCA AAT-3′; reverse, 5′-GTG GAT ACA TAC AAG AGA GAC TTT GTC CC-3′, 173 bp), *HIST1H3B* (forward, 5′-CTG CTC GTA AGT CCA CCG GTG-3′; reverse, 5′-GCG ATC TCC CTC ACC AAC CTC-3′, 243 bp), *TERT* promotor (forward 1, 5′-GTC CTG CCC CTT CAC CTT-3′; reverse 1, 5′-GCA CCT CGC GGT AGT GG-3′, 273 bp; forward 2, 5′-CCG TCC TGC CCC TTC ACC-3′; reverse 2, 5′-GGG CCG CGG AAA GGA AG-3′, 128 bp), and *BRAF* (forward, 5′-TCA TAA TGC TTG CTC TGA TAG GA-3′; reverse, 5′-GGC CAA AAA TTT AAT CAG TGG A-3′, 223 bp). Standard buffer conditions, 50 ng of DNA, and Taq DNA Polymerase (TaKaRa) were used. The reaction mixture was subjected to an initial denaturation at 95°C for 10 min, followed by 35 cycles of amplification (denaturation at 95°C for 30 s, annealing at 56°C for 30 s, and extension at 72°C for 40 s). PCR products were purified using a MinElute PCR Purification Kit (Qiagen, Hilden, Germany) and were sequenced in both sense and antisense directions using an automated sequencer (ABIPRISM 3100 Genetic Analyzer; Applied Biosystems, Waltham, MA, USA).

Table 1 Results of immunohistochemistry in these three cases

Antigen	Case 1	Case 2	Case 3
GFAP	+	+	+
Oligo2	+	+	+
IDH1 R132H	–	–	–
ATRX	+	+	+
NeuN	–	–	–
EMA	–	–	–
H3K27M	–	–	–
p53 labeling index	30%	5%, weak	1%, weak
Ki-67 labeling index	40%	30%	25%

MGMT promoter methylation

Total DNA was extracted from FFPE sections for bisulfite conversion. A EZ DNA Methylation-Gold Kit (Zymo Research, CA, USA) was used according to the manufacturer's instructions. The *MGMT* methylation status was assessed with a methylation-specific PCR, which was performed using PCR primer sets specifically for methylated

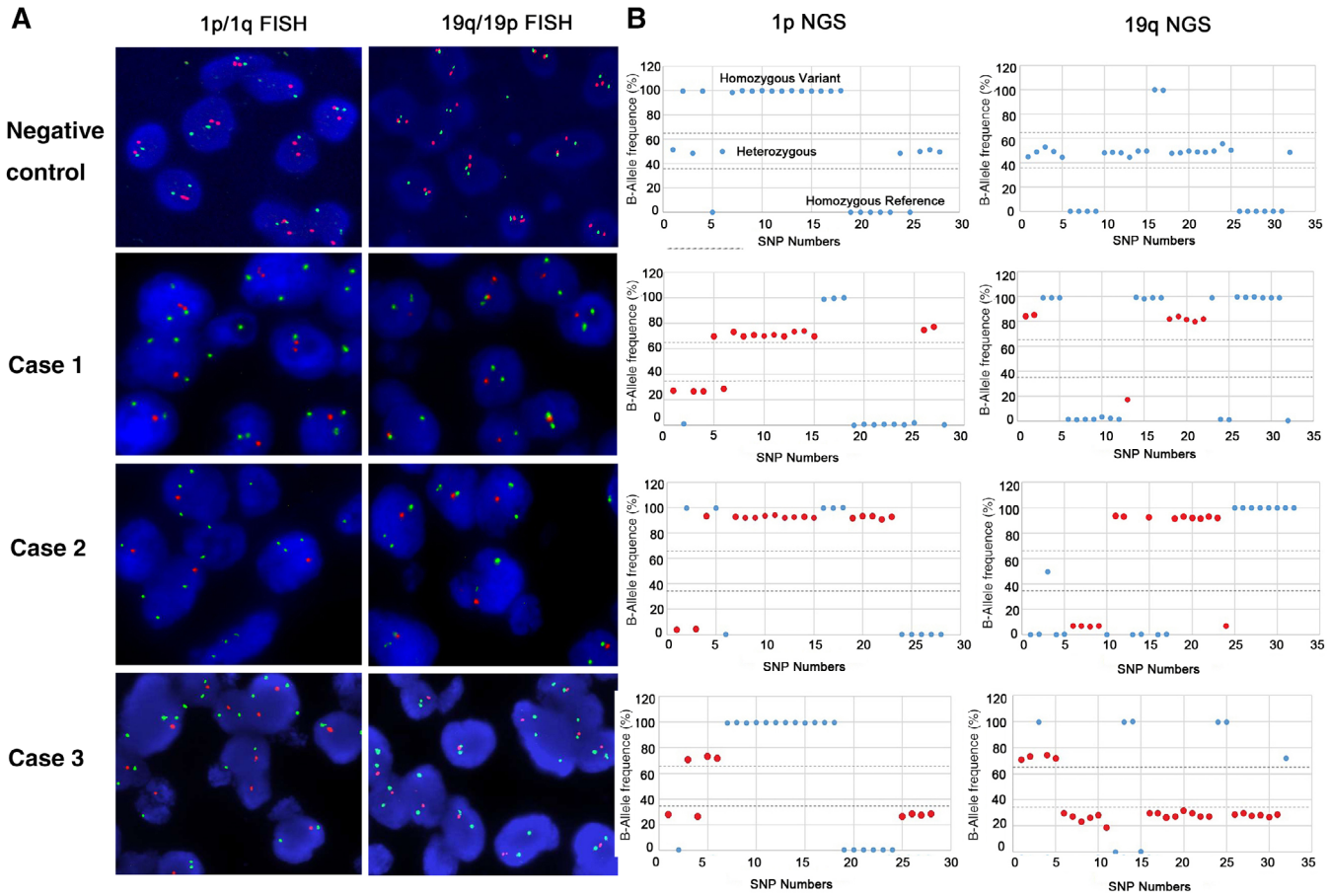

Fig 5 FISH analysis of 1p/19q codeletion (A) and NGS-based NSPs (B) analyses. (A) The upper line shows the control of no deletion of 1p or 19q signals. The lower three lines show the 1p/19q codeletion in our three cases. Red dots represent 1p and 19q signals, and green dots represent 1q and 19p signals. (B) The x-axis shows the numbers of the selected SNP sites, and the y-axis shows the percentage variant (B-allele frequency). Blue dots reflect a normal pattern, and red dots reflect aberrant bi-allele frequency. The upper line shows the distribution of B-allele frequencies of chromosome 1p and 19q SNPs of normal brain tissues. The lower three lines show allelic losses and imbalances of chromosomes 1p and 19q SNPs in our three cases, indicating 1p/19q codeletion.

and unmethylated *MGMT* promoter sequences: *MGMT*-methylated, 5′-TTT CGA CGT TCG TAG GTT TTC GC-3′, 5′-GCA CTC TTC CGA AAA CGA AAC G-3′ and *MGMT*-unmethylated, 5′-TTT GTG TTT TGA TGT TTG TAG GTT TTT GT-3′, 5′-AAC TCC ACA CTC TTC CAA AAA CAA AAC A-3′.

Table 2 Genetic alterations of these three cases

Target	Case 1	Case 2	Case 3
1p/19q codeletion	+	+	+
IDH1 (R132) mutation	–	–	–
IDH2 (R172) mutation	–	–	–
TERT promotor 228 mutation	–	–	–
TERT promotor 250 mutation	–	–	–
H3F3A (K27) mutation	–	–	–
H3F3A (G34) mutation	–	–	–
HIST1H3B (K27) mutation	–	–	–
HIST1H3B (G34) mutation	–	–	–
BRAF (V600) mutation	–	–	–
MGMT promotor methylation	–	+	–

RESULTS

Neuropathological findings

Histologic examination of all the three cases revealed a high degree of cellular and nuclear pleomorphism with appearance of numerous multinucleated giant cells and brisk mitotic activity. Prominent microvascular proliferation was seen in all the cases, and palisading necrosis was observed in case 3 but not in cases 1 and 2. An oligodendroglioma-like component was also observed in cases 2 and 3 but not in case 1. In case 2, a specific structure of neuropil-like island was scattered in tumor cells. Representative morphology is shown in Figures 2, 3, and 4.

Immunohistochemically, the tumor cells in all cases were strongly positive for GFAP and Oligo2. ATRX was retained in the cell nuclei. IDH1 R132H, EMA, NeuN, and H3 K27M were negative in all cases. The tumor cells had a high proliferative activity based on the Ki-67 labeling index from 25% to 40%, and approximately 5% to 30% of the tumor cells were weakly positive for p53 in different cases. Immunohistochemistry for molecular alterations in cases 1, 2, and 3 are summarized in Table 1 and Figures 2, 3, and 4.

1p/19q codeletion was confirmed in all three cases by both FISH analysis (Fig. 5A) and NGS-based SNPs analysis (Fig. 5B). No hot site mutation was detected in other molecular analyses, including *IDH1* (R132), *IDH2* (R172), *H3F3A* (K27 and G34), *HIST1H3B* (K27 and G34), *BRAF* (V600), and *TERT* promotor (228 and 250). Based on methylation-specific PCR, *MGMT* promotor methylation was detected in case 2 but not cases promotor 1 and 3. The genetic alterations are summarized in Table 2.

DISCUSSION

The WHO 2016 classification tumors of the CNS broke the traditional classification by using molecular-genetics data to separate different gliomas. It was hoped that the new classification would provide clearer indication of tumor behavior using molecular-genetic criteria rather than previous grading criteria based on morphology alone. Using the new classification, oligodendroglioma is diagnosed only if harboring both *IDH1* or *IDH2* mutation and 1p/19q codeletion. If the *IDH* is wild-type based on results obtained by both immunohistochemistry and DNA sequencing, a 1p/19q FISH test is not recommended. As a result, it was not easy to find gliomas with *IDH* wild-type and 1p/19q codeletion and few studies have been done so far. It is still unknown whether this kind of glioma is an independent entity or belongs to a certain glioma subtype.

The WHO classification does not suggest which method should be used to detect 1p/19q codeletion, but points out that whole-arm chromosomal losses should be detected. The existing methods for 1p/19q assessment include FISH, chromogenic *in situ* hybridization (CISH), PCR-based microsatellite analysis, array comparative genomic hybridization (CGH), multiplex ligation-dependent probe amplification (MLPA), SNP arrays, and NGS.[18] FISH is one of the most common methods used to evaluate loss of 1p and19q, especially in hospitals. The advantage of FISH was that it could preserve the architecture of tissue and cytological features, and that the evaluation was based on morphology. The disadvantage was that its probes could not cover the whole arm of the chromosome, and that it was unable to discriminate between full-arm and partial deletions. In contrast, other methods like PCR-based microsatellite analysis, CGH, MLPA, SNP arrays, and NGS could assess the whole arm losses of 1p and 19q, but not *in situ*. To ensure the accuracy of the results, we used both FISH analysis and NGS-based SNP analysis to assess the status of chromosomes 1p and19q and confirmed 1p/19q codeletion in our cases.

Although most studies have illustrated that typical 1p/19q loss is always associated with *IDH* mutations,[12,13] at least eight gliomas with 1p/19q codeletion and *IDH* wild-type have been reported.[14–16] From two recent large-scale molecular genetics studies on diffuse gliomas reclassification according to the 2016 new classification, only four of 1041 gliomas[14] and two of 1206 gliomas[15] were identified with these atypical molecular changes. However, they were excluded when being reassigned for the atypical molecular phenotype without further comprehensive molecular analysis. In another study on the reclassification of 82 gliomas, two tumors of 1p/19q codeleted and *IDH* wild-type were reassigned to oligodendroglioma, NOS.[16]

In this study we report three high-grade gliomas with 1p/19q codeletion but without *IDH1/2* hot site mutation, based on the results obtained by both immunohistochemistry and DNA sequencing; they were gray cases according to the revised WHO classification. It is well known that high cellularity, cellular pleomorphism, prominent microvascular proliferation, and/or palisading necrosis are essential diagnostic features of GBM. In the present study, high degree of cellular and nuclear pleomorphism and microvascular proliferation were seen in all cases, but typical palisading necrosis was seen only in case 3. Some oligodendroglioma-like area was seen in cases 2 and 3, resulting in diagnosis as having anaplastic oligodendroastrocytoma or glioblastoma with an oligodendroglioma component (GBMO) according to the 2007 morphological criteria. We then comprehensively tested other glioma-related genetic parameters in these three cases. ATRX were retained, the p53 labeling index was very low, and p53 immunoreactivity was relatively weak in these cases. Neither hot site mutation was detected in *H3F3A, HIST1H3B, BRAF*, and *TERT* promoter in all the cases. *MGMT* promoter methylation was confirmed in case 2, and no methylation was detected in case 1. Cases 1 and 2 had relatively poor outcomes, like GBM. Taking these pathological and molecular features and biological behaviors into consideration, we concluded that these rare tumors were not atypical GBMs but were closer to GBMs than anaplastic oligodendrogliomas.

In conclusion, we reported a specific type of high-grade glioma with uncommon molecular phenotype, which harbored 1p/19q codeletion but without *IDH1/2* hot site mutation, based on results obtained by both immunohistochemistry and DNA sequencing. The gliomas could not be

categorized according to the molecular-genetic criteria of the 2016 revision of the WHO classification of tumors of the CNS. Considering the morphology and other molecular parameters as well as patients' prognosis, we found that these gliomas were more likely to be GBMs than anaplastic oligodendrogliomas. However, more cases are needed for accurate classification of this rare tumor.

DISCLOSURE

The authors declare no conflict of interest.

ACKNOWLEDGMENT

Support was received through grants from the National Natural Science Foundation of China (NSFC 81872107, 81872108, 81572540, and 81572541).

REFERENCES

1. Omuro A. Glioblastoma and other malignant gliomas: A clinical review. *JAMA* 2013; **310**: 1842–1850.
2. Louis DN, Ohgaki H, Wiestler OD. *WHO Classification of Tumours of the Central Nervous System*. Lyon: IARC Press, 2007.
3. Komori T. The 2016 WHO classification of tumours of the central nervous system: The major points of revision. *Neurol Med Chir* 2017; **57**: 301–311.
4. Louis DN, Ohgaki H, Wiestler OD. *WHO Classification of Tumours of the Central Nervous System*, revised 4th edn. Lyon: IARC Press, 2016.
5. Eckel-Passow JE, Lachance DH, Molinaro AM et al. Glioma groups based on 1p/19q, IDH, and TERT promoter mutations in tumors. *N Engl J Med* 2015;**372**: 2499–2508.
6. Brat DJ, Verhaak RG, Aldape KD *et al*. Comprehensive, integrative genomic analysis of diffuse lower-grade gliomas. *N Engl J Med* 2015; **372**: 2481–2498.
7. Suzuki H, Aoki K, Chiba K et al. Mutational landscape and clonal architecture in grade II and III gliomas. *Nat Genet* 2015;**47**: 458–468.
8. Weller M, Weber RG, Willscher E et al. Molecular classification of diffuse cerebral WHO grade II/III gliomas using genome- and transcriptome-wide profiling improves stratification of prognostically distinct patient groups. *Acta Neuropathol* 2015;**129**: 679–693.
9. Mollemann M, Wolter M, Felsberg J, Collins VP, Reifenberger G. Frequent promoter hypermethylation and low expression of the MGMT gene in oligodendroglial tumors. *Int J Cancer* 2005; **113**: 379–385.
10. Jiao Y, Killela PJ, Reitman ZJ et al. Frequent ATRX, CIC, FUBP1 and IDH1 mutations refine the classification of malignant gliomas. *Oncotarget* 2012; **3**: 709–722.
11. Chaurasia A, Park SH, Seo JW, Park CK. Immunohistochemical analysis of ATRX, IDH1 and p53 in glioblastoma and their correlations with patient survival. *J Korean Med Sci* 2016; **31**: 1208–1214.
12. Dubbink HJ, Atmodimedjo PN, Kros JM et al. Molecular classification of anaplastic oligodendroglioma using next-generation sequencing: A report of the prospective randomized EORTC Brain Tumor Group 26951 phase III trial. *Neuro Oncol* 2016;**18**: 388–400.
13. Labussiere M, Idbaih A, Wang XW et al. All the 1p19q codeleted gliomas are mutated on IDH1 or IDH2. *Neurology* 2010;**74**: 1886–1890.
14. Tabouret E, Nguyen AT, Dehais C *et al*. Prognostic impact of the 2016 WHO classification of diffuse gliomas in the French POLA cohort. *Acta Neuropathol* 2016; **132**: 625–634.
15. Pekmezci M, Rice T, Molinaro AM et al. Adult infiltrating gliomas with WHO 2016 integrated diagnosis: Additional prognostic roles of ATRX and TERT. *Acta Neuropathol* 2017;**133**: 1001–1016.
16. Rogers TW, Toor G, Drummond K et al. The 2016 revision of the WHO classification of central nervous system tumours: Retrospective application to a cohort of diffuse gliomas. *J Neurooncol* 2018;**137**: 181–189.
17. Dubbink HJ, Atmodimedjo PN, van Marion R et al. Diagnostic detection of allelic losses and imbalances by next-generation sequencing: 1p/19q co-deletion analysis of gliomas. *J Mol Diagn* 2016; **18**:775–786.
18. Woehrer A, Hainfellner JA. Molecular diagnostics: Techniques and recommendations for 1p/19q assessment. *CNS Oncol* 2015; **4**: 295–306.